M. BENZAGHTA

ATILIM UNIVERSITY

MODELING AND MEASUREMENT OF RECEIVED SIGNAL VARIABILITY OVER POPULATED LINKS IN INDOOR CHANNELS AT MMWAVES

THE GRADUATE SCHOOL OF NATURAL AND APPLIED SCIENCES
OF
ATILIM UNIVERSITY

MOHAMED BENZAGHTA

A MASTER OF SCIENCE THESIS
IN
THE DEPARTMENT OF ELECTRICAL AND ELECTRONICS ENGINEERING

APRIL 2021

MODELING AND MEASUREMENT OF RECEIVED SIGNAL VARIABILITY OVER POPULATED LINKS IN INDOOR CHANNELS AT MMWAVES

A THESIS SUBMITTED TO
THE GRADUATE SCHOOL OF NATURAL AND APPLIED SCIENCES
OF
ATILIM UNIVERSITY

BY

MOHAMED BENZAGHTA

IN PARTIAL FULFILLMENT OF THE REQUIREMENTS
FOR
THE DEGREE OF MASTER OF SCIENCE
IN
THE DEPARTMENT OF ELECTRICAL AND ELECTRONICS ENGINEERING

APRIL 2021

Approval of the Graduate School of Natural and Applied Sciences, Atilim University.

_____

Prof. Dr. Ender KESKİNKILIÇ
Director

I certify that this thesis satisfies all the requirements as a thesis for the degree of **Master of Science in Electrical and Electronics Engineering Department, Atilim University**.

_____

Assoc. Prof. Kemal Efe ESELLER
Head of Department

This is to certify that we have read the MODELING AND MEASUREMENT OF RECEIVED SIGNAL VARIABILITY OVER POPULATED LINKS IN INDOOR CHANNELS AT MMWAVES submitted by MOHAMED BENZAGHTA and that in our opinion it is fully adequate, in scope and quality, as a thesis for the degree of Master of Science.

_____

Prof. Dr. Ali KARA
Supervisor

Examining Committee Members:

Asst. Prof. Dr. Özgür Ergül
Electrical and Electronics Eng. Dept., Gazi University _____

Prof. Dr. Ali Kara
Electrical and Electronics Eng. Dept., Gazi University _____

Prof. Dr. Bülent Tavlı
Electrical and Electronics Eng. Dept., TOBB-ETU _____

Prof. Dr. Elif Aydin
Electrical and Electronics Eng. Dept., Atilim University _____

Asst. Prof. Dr. Mehmet Efe Özbek
Electrical and Electronics Eng. Dept., Atilim University _____

Date: 12/04/2021

I hereby declare that all information in this document has been obtained and presented in accordance with academic rules and ethical conduct. I also declare that, as required by these rules and conduct, I have fully cited and referenced all material and results that are not original to this work.

Name, Last Name: Mohamed Benzaghta

Signature:

ABSTRACT

MODELING AND MEASUREMENT OF RECEIVED SIGNAL VARIABILITY OVER POPULATED LINKS IN INDOOR CHANNELS AT MMWAVES

Benzaghta, Mohamed
M.S., Department of Electrical and Electronics Engineering
Supervisor: Prof. Dr. Ali Kara

April 2021, 40 pages

Millimeter-wave (mm-wave) spectrum is an essential enabler to the fifth generation (5G) wireless technology. In using mm-wave spectrum based communication links, humans are one of the most noticeable blockers that cause temporal variation in the radio channel. This thesis presents human blockage measurements at 28GHz investigating 3 human subjects of different size. Also the effect of the human blockage crossing orientation is investigated by this study taking into account 3 different transmitter heights of 1m, 1.3m and 1.6m. An effective human blockage model based on Fresnel diffraction scheme is shown to accurately estimate the blockage loss by fitting the measurements precisely, considering different human body dimensions, different crossing orientations, as well as different antenna heights. The Fresnel diffraction human blockage model is also compared to the geometrical theory of diffraction (GTD) human blockage model, and is found to be more accurate while using less computational efforts. Furthermore, this thesis presents indoor propagation measurements for an office environment short-range communication link at 28GHz in the presence of human activities. The human blockage activities are characterized in terms of the blockage duration, maximum temporal fading, and overall path loss. The experimental results considering 3 to 6 humans' activities for 3 different antenna

height combinations are reported and empirical models are proposed accordingly to characterize the small-scale fading from a link blockage point of view.

Keywords: Radio propagation, human body shadowing, millimeter waves, signal fading, fifth-generation (5G) networks.

ÖZ

MİLİMETRE DALGA BANDINDA BİNA İÇİ-İNSAN YOĞUN ORTAMLARDA SİNYAL SEVİYESİ DEĞİŞKENLİĞİNİN ÖLÇÜMÜ VE MODELLENMESİ

Benzaghta, Mohamed

Yüksek Lisans, Elektrik ve Elektronik Mühendisligi

Tez Yöneticisi : Prof. Dr. Ali KARA

Nisan 2021, 40 sayfa

Milimetre dalga spektrumu, beşinci nesil (5G) kablosuz teknoloji için en temel bileşendir. Milimetre dalga bandındaki radyo kanallarında insan vücudu önemli kesinti sebebi ve sinyal değişkenliği nedenidir. Bu tez çalışmasında, 28 GHz bandında 3 farklı insan modeli ile insan vücudunun sinyal kesintisine ve zayıflamasına etkisine yönelik ölçümler sunulmaktadır. Ayrıca farklı alıcı-verici anten yüksekliklerine göre insan vücudu yerleşiminin etkisi de incelenmektedir. Farklı boyutlarda insan vücutları ve yerleşimleri ile anten yükseklikleri dikkate alınarak Fresnel kırınım modelinin en iyi çalışan model olduğu gösterilmektedir. Ayrıca Fresnel kırınım modeli ile Geometrik Kırınım Teorisi (GKT) modellerini de kıyaslanmakta, öncekinin daha doğru ve gerçeklenmesi basit olduğu gösterilmektedir. İlave olarak tez çalışmasında, insan yoğunluğunun milimetre dalga yayılımında kesinti süresi ve derinliğine yönelik istatistiklerde ölçümler yoluyla çıkarılmaktadır. Bu kapsamda, 3 ve 6 kişinin bir ofis ortamında olağan günlük hareket rotaları dikkate alınarak radyo linkini kesmesine yönelik istatistikler ilk defa bu tez çalışmasında sunulmaktadır.

Anahtar Kelimeler: Radyo yayılımı, insan vücudu etkisi, milimetre dalgalar, sinyal zayıflaması, beşinci nesil (5N) ağlar,

To the ones keen on Science, Research and Knowledge

ACKNOWLEDGMENTS

The author sincerely expresses his deepest gratefulness to the Almighty God (Allah). I hope He blesses this work as an ongoing charity and a beneficial knowledge for the sake of humanity.

First and foremost, the author would like to express his sincere thanks to his supervisor Prof. Dr. Ali Kara. His passion towards research and the ambitious for discovering solutions regarding human blockage effects at mmWave frequency bands had been the key to successfully completing this thesis. He has always been a tremendous mentor.

This thesis study was financially supported by Atilim University under LAP Grant (ATU-LAP-2021-02). The author would also like to thank all of the students and colleagues who volunteered as human models for the experimental measurements.

The author would also like to thank the assistance and encouragement of his dear friends that had a vital role toward completing this study.

Finally, the author wishes to express his deepest thankfulness and appreciation to his father (Dr. Mostafa), mother (Naima), and my siblings (Loai and Ali) for their believe in me, encouragement, their continues support, and for their sacrifice throughout my entire educational journey.

TABLE OF CONTENTS

LIST OF TABLES

TABLES

LIST OF FIGURES

FIGURES

LIST OF SYMBOLS/ABBREVIATIONS

3GPP	Third-generation partnership project
4G	Fourth generation cellular technology
5G	Fifth generation cellular technology
CDF	Cumulative Distribution Function
DKED	Double Knife-edge Diffraction
DTMKE	Double-truncated multiple knife-edge
Gbps	Gigabit-per second
GTD	Geometrical Theory of Diffraction
IoT	Internet-of-Things
LOS	Line-of-sight
MIMO	Multiple-input Multiple-output
MKED	Multiple Knife-edge Diffraction
Mm-Wave	millimeter-wave
PDF	Probability Density Function
Rx	Receiver
SE	Shadowing Event
Tx	Transmitter
UTD	Uniform Theory of Diffraction

CHAPTER 1

INTRODUCTION

1.1. Research Background

Wireless data traffic is increasing at a significant rate over the past few years, and it is expected to experience a further increase in the coming decade. This is mainly due to the continual rise of smartphones usage, video streaming and the increasing demand on Internet-of-Things (IoT) applications [1]. The current used sub-6GHz spectrum is unable to afford this increasing demand in bandwidth and spectral efficiency. Therefore, in order to overcome the global bandwidth shortage, the wireless industry is establishing the fifth generation cellular technology (5G) that is going to employ the millimeter-wave (mm-Wave) frequency spectrum [2].

The movement toward using the mm-Wave spectrum is expected to tackle the exponential growth of the predicted data traffic capacities by providing channel bandwidths of more than ten times larger than nowadays fourth generation (4G) cellular channels, as well as supporting multi-Gigabit-per second (Gbps) data rates [3]. However, as the wavelengths of mm-Wave frequency bands are less by an order of magnitude when compared to microwave frequency bands that are used in today's 4G systems, then the propagation characteristics of those frequency bands are impacted greatly by small obstacles [4-6]. Consequently, the penetration and diffraction caused by human blockages will suffer from a greater attenuation, and the movement of human bodies around the propagation link will lead to temporal variations in the radio channel [7, 8]. Given the vision that mm-Wave communication systems will be deployed in urban streets and open squares, as well as indoor environments, the third-generation partnership project (3GPP) has considered humans to be identified as one of the major obstacles that affect the mm-Wave propagation channel [9]. This requires precise evaluation of the human blockage loss by providing accurate models having

low complexity of human body geometrical description and reduced computations. Also, propagation models that can predict the variations of the radio channel as people move about the link are needed.

The human blockage models that are available in the literature [10–25] evaluate the loss due to the human blockage by taken into account the body dimensions and shape. Although these proposed models provide good accuracy at cost of complexity in the human body geometrical representation and increase computations, these proposed models are not comprehensively validated for different body sizes (height, width. and thickness of the human model), orientation (the angle of which the human body blocks the signal), and antenna height dependence. Moreover, little is known about the behaviour of the mm-Wave radio signals under the effect of human blockage, as users move about the propagation link, especially in indoor areas. This information is considered to be vital for the design of future mm-Wave communication systems that can overcome the deep fades due to the human blockage loss by designing suitable handoff mechanisms and beam steering techniques.

1.2. Aim and Objectives of the study

The key contributions of this thesis can be summarized as:

1) A detailed comprehensive literature survey is provided to review the human blockage models proposed for estimating the blockage loss, as well as reviewing the reported work on the small-scale behaviour of mmWave signals when users move near the local area propagation link for indoor scenarios.

2) The human blockage loss measurements at 28GHz based on three human models of different heights and widths, two different crossing orientations of the Line-of-sight (LOS), and the use of three different transmitter height are reported.

3) A simple yet an accurate human blockage model based on Fresnel diffraction method, that is proven to be valid for different body heights, and widths, different orientations, as well as different antenna heights is proposed.

4) Empirical models based on experimental propagation measurements investigating the small-scale fading behaviour of mm-Wave signals due to the effect of human blockages movement nearby the propagation link at 28GHz, for real life indoor environment scenarios are presented.

1.3. Thesis Structure

This thesis is organized as follows: Chapter 2 provides a comprehensive literature review on the human blockage loss and the proposed theoretical models, as well as providing a review on the small-scale behaviour of mmWave signals due to human blockage movements for indoor environments. Chapter 3 presents the blockage loss measurements at 28GHz performed on 3 different human models having different body sizes, combined with different crossing orientations and antenna heights. A simple and accurate human blockage model is also given in this section. Chapter 4 reports the experimental measurements for investigating the effect of human blockage movements on the propagation characteristics at 28GHz for indoor environments. Empirical models based on the measurements are also proposed in this section. Finally, in Chapter 5 this thesis is summarized and conclusions are drawn.

CHAPTER 2

COMPREHENSIVE LITERATURE REVIEW

Several studies are proposed in literature for determining the blockage loss due to humans, based on the shape and dimensions of the body. These models use simplified mathematical formulations which are mainly based on the concept of diffracted rays around the blocking object. An important parameter in modelling the human blockage is choosing a suitable geometrical representation of the human body such as shape, and dimensions. In this thesis, we provide a deeper insight on those proposed models in terms of their use and accuracy for the mm-Wave frequency band (reported literature on frequency bands of less than 28GHz is not included in this survey), taking into consideration the human body dimensions, orientation of the blockage object and the effect of the antenna height on the blockage loss. Furthermore, an additional literature survey is provided regarding the reported work on the behaviour of mm-Wave signals effected by the movement of humans near the propagation link for indoor environments.

In [12], the authors presented human blockage loss measurements at 73GHz for an indoor environment having 5m separation distance between the transmitter (Tx) and the receiver (Rx). The human model in this experiment walked in a perpendicular orientation to the propagation link between the Tx and the Rx with a speed of approximately 1m/s. It was observed that an average size human body can lead to a blockage loss of 30-40dB and a blockage duration of 200 ms to 300 ms. Double Knife-edge Diffraction (DKED) model was used to model the blockage loss by modelling the human body as rectangular screen having an infinite vertical height. The reported results show that the proposed model underestimates the measured loss by approximately 10dB.

Measurements of human blockages in an anechoic chamber were also performed in [10] at 60GHz and 28GHz. In this study, 15 different human models were located at

the midpoint of the Tx and Rx antennas separation. A double-truncated multiple knife-edge (DTMKE) model was proposed to fit the measurements. It was observed that the loss increases as the frequency increases, which were recorded to have an average increase of 7–10 dB more at 60GHz. Human blockage loss at 60GHz for static scenarios where a human body is blocking the LOS without movement in an anechoic chamber was also measured by [13]. It was found from this study that the blockage loss can reach up to 20dB. The authors in [14] also analysed the shadowing loss due human body at 60GHz, using a 2x2 Multiple-input Multiple-output (MIMO) channel measurement campaign. The DKED and the Uniform Theory of Diffraction (UTD) were used to estimate the blockage loss. It was seen that the DKED underestimates the loss, whereas the UTD overestimates it. The human model in this study crossed the LOS in a frontal manner with a speed of approximately 0.5m/s. In [15], the authors investigated the blockage loss at both 60GHz and 300GHz. The distance between the Tx and Rx was 2.7m at 60GHz and 1m at 300GHz. The human model crossed the LOS with a speed of between 0.9-1.2 m/s. The DKED model was used to model the blockage loss measurement. It was observed that the model estimates the loss better at 60GHz when compared to 300GHz, with a difference of more than 15dB in accuracy between the proposed model and the measurements at 300GHz. Comparing different geometrical models for estimating the blockage of the LOS was done in [16], in which the authors compared both MKED and UTD models at 60GHz. It was found that UTD is more accurate; however, when considering the computational effort, the MKED was found to be more efficient. A Gaussian statistical model was proposed in [17] for characterizing the blockage event of human bodies at 60GHz. Two human models were used to simulate realistic scenarios for intercepting the LOS path in a random manner with a speed of about 1 m/s. It was seen that the received power effected by the human blockage can follow a Gaussian statistical distribution. Additionally, the blockage loss caused by several human bodies at 60GHz was investigated in [18]. It was observed that when the blockage event involves three human blockers, then the loss can reach up to 50dB for antenna heights of 1m at this mm-Wave frequency band. Instead of using real human bodies, a variety of phantoms were proposed in [19] to simulate the human blockage loss at 60GHz. Four different objects were considered and it was found that water-filled human phantom served as a suitable approximation for the human body.

In [20], the authors studied the effect of the human skull and body blockage loss at 38GHz. The human body blocked the LOS at a distance of 0.2m from the Rx. It was found that the loss due to the skull can reach up to 22dB, whereas the loss of the body can be around 32dB. The KED model can be used in modelling the worst case estimated loss based on the measured results. In [11], the blockage loss due to a human body was investigated at 32GHz and 28GHz. The measurements were performed in an indoor office environment where a person is crossing the LOS, as well as walking in parallel with the LOS. The METIS model, Geometrical Theory of Diffraction (GTD), and the Gaussian model were used to simulate the human blockage effects. It was observed that when the frequency increases, there is no increase in the losses between 28GHz and 32GHz and the losses are usually between 15-30dB.

Regarding the measurements at 28GHz, the authors in [21] investigated the blockage loss due to humans in the case of lateral crossing scenarios, as well as non-crossing situations similar to [12]. It was seen that the measured loss can range between 6-16dB with a shadowing distance of 0.4-0.8m. DKED and Multiple-edge Diffraction Methods (MKED) were used to validate the results. The difference between the simulated and the measured results differ by 1-4dB for the given specific crossing scenario. Measurements using real-time channel sounder to study the human blockage loss at 28GHz was also done in [22]. The separation distance between the Tx and the Rx was set to 5m and 10m, and the human model crossed the LOS at 2.5m and 1.25m from the Tx. The speed of the pedestrian was approximately 1.4m/s. Comparisons of high directional antennas with sectoral-wide ones was investigated in this study. It was found that the sectoral-wide beam has a 9 dB less loss than the directional beam. The reason is that the human body is fully blocking the propagation link when using directional antennas. An experimental study reported in [23] investigated the blockage loss at 28GHz for antenna heights of 1.2m and 1.4m. A separation distance of 10m between the antennas were used in the measurements. It was observed that the maximum loss occurs when the human is near either the transmitter or the receiver and this loss decreases to its minimum value at the midpoint of the separation distance. The experiment revealed that the body blockage loss varies in range of 10–36dB. The authors in [24, 25] presented the effect of human blockages nearby indoor links at 28GHz for Non-LOS scenarios, in which the LOS is fully blocked by a human body. The DKED model was proposed in [25] to estimate the loss due to one human body,

whereas in [24] the street canyon propagation model was proposed to predict the loss due to two human bodies approaching the link. The human body in those studies was considered to be scattering objects. It was observed that the loss is lower when the human is 0.8m away from the link (1-3dB). The DKED model has less accuracy when compared to the street canyon propagation model; however, it is less complex in terms of computational efforts. A detailed summary of the published literature on human body blockage at mm-Wave frequency bands is provided in Table. 2.1.

Table 2.1 Literature Survey

Frequency	**Ref.**	**Proposed Model**	**Validation of the model**		
			Number of human models	**Number of investigated crossing orientation**	**Number of Antenna Height combinations**
300GHz	[15]	DKED	1 (Height not given and Width=0.31m)	1 (Crossing orientation is not given)	1 (Tx=Rx= 1.1m)
73GHz	[12]	DKED using infinite vertical height.	1 (Height=1.80m and Width=0.47m)	No crossing (The human model is walking along the LOS path)	1 (Tx=Rx= 1.4m)
60GHz	[10]	DTMKE	15 different human models	No crossing	Tx is raised from 1.87 to 3.07 m in steps of 0.15 m
	[13]	KED	1 (Height not given and Width=0.5m)	No crossing	1 (Tx=Rx= 1.1m)

Table 2.1 Literature Survey (Continued)

60GHz	[14]	DKED and UTD	1 (Height not given and Width=0.56m)	1 (Frontal crossing)	1 (Tx=Rx= 1.2m)
	[16]	MKED and UTD	1 (Height and width are not given)	No crossing	1 (Tx=Rx= 1.1m)
	[17]	Gaussian statistical model	2 (Heights and widths are not given)	Random Crossings	Not given
	[18]	DKED using infinite height.	3 (Heights are not given and Width ranging from 0.43 to 0.48m)	1 (Frontal crossing)	1 (Tx=Rx= 1m)
39.5GHz	[34]	MKED	3 (Heights are not given and widths are 0.48, 0.49, 0.5m)	2 (Lateral and Frontal crossing)	1 (Tx=Rx= 1.3m)
38GHz	[20]	KED	1 (Height and width of the model are not given)	No crossing	2 (Tx=Rx= 1.25m and Tx=Rx=1.5 m)
32GHz	[11]	METIS, GTD, and the Gaussian model	2 (same dimensions, Height=1.80m and Width=0.40m)	1 crossing scenario and a non-crossing scenario	1 (Tx=Rx= 1.4m)

Table 2.1 Literature Survey (Continued)

28GHz	[21]	DKED and MKED	1 (Height=1.72m and Width=0.43m)	1 (Lateral crossing) and a non-crossing scenario	1 (Tx=Rx= 1.3m)
	[22]	No model proposed	2 (same dimensions, Height=1.76m, Width is not given)	1 (Lateral crossing)	1 (Tx=1.55, and Rx=1.65m)
	[23]	No model proposed	4 (Height ranging from 1.74m to 1.83m, Width is not given)	No crossing	2 (Tx=Rx= 1.2m and Tx=Rx=1.4 m)
	[25]	DKED	1 (Height is not given and Width=0.47m)	No crossing	1 (Tx=Rx= 1m)
	[24]	Street canyon propagation model	2 (Heights are not given and Widths are 0.5m and 0.48m)	No crossing	1 (Tx=Rx= 1m)
	This Thesis	Fresnel Diffraction model using finite dimensions	3 (Heights of 1.66m, 1.73m and 1.88m, and widths of 0.40m, 0.44m, and 0.48m)	2 (Lateral and Frontal crossing)	3 (Tx=Rx= 1m, Tx=1.3m with Rx=1m, and Tx=1.6m with Rx=1m)

All of the previously reported literature [10-25] examined only static pre-defined scenarios, where the blockage loss is measured either for lateral crossing, frontal crossing or no crossing of LOS cases. These study cases do not represent real-life daily indoor scenarios, in which several humans are randomly moving within a specific area. In literature, only a few studies [26-33] examined the effect of human blockage movements on the behaviour of mm-Wave signals for indoor environments.

Most of the reported experimental studies were performed at the mm-Wave frequency band of 60GHz. In [26], indoor propagation measurements were done in a large working room in presence of human activity for up to 15 persons. The human blockage effect was characterized in terms of total blockage loss and duration. It was observed that the total blockage loss is more than 20dB, having a duration in range of 100-300ms. Similar fading durations were reported by [27]; however, deeper fades reaching up to 48dB were recorded. It should be noted that the measurement environment for these studies were not identical. In [28], the authors' investigated the effect of human blockage movements, varying from 1 to 3 persons, in a home environment for a gaming/streaming scenario. It was reported that the loss due to human activities in such scenarios can reach up to 40dB. The recent empirical outcomes given by [29] characterized the fades caused by pedestrians in indoor areas where 60GHz WiGig access points are deployed. In average, the fades were found to be 21dB with duration lasting up to 5s. Also, empirical results for measuring the blockage loss due to 2 and 5 persons' activities in an indoor empty room at 66.5GHz were reported in [30]. The blockage loss was approximately 22dB for 2 persons' activities and 29dB for 5 persons for antenna height of 2m.

A ray tracing simulation approach was presented in [31, 32]. The simulations were based on stochastic human blockage models considering multiple humans. Realistic indoor scenarios were achieved without any significant increase in the complexity of the model. It was observed that as the number of humans increase the blockage loss increases significantly; however, the delay spread decreases. Tractable statistical simulation models accounting for human body blockages for office scenarios were also presented in [33]. Accurate human blockage events characterizations based on regression fits were given. Mm-wave frequency bands of 54-59GHz and 61-66GHz were considered in the simulations.

CHAPTER 3

HUMAN BLOCKAGE MODEL

Most of the reported literature on determining the human body blockage effect simulate the human body geometry by the use of either a rectangular absorbing screen (based on KED method) or a perfectly conducting cylinder (based on GTD method). In this paper we present the use of Fresnel diffraction method to estimate the effect of the human blockage by considering multiple diffractions.

3.1 Method of Calculating Human Body Shadowing Gain

The human body geometrical model is represented as a rectangular plate given in Fig. 3.1. The ray going from the Tx to the Rx crosses the plate at a certain point. The shortest distances between the edges of the plate and the ray crossing point are denoted as H_{b1} and H_{b2}. The distance from the human model to the Tx is denoted as D_{tp}, whereas the distance to the Rx is defined by D_{rp}. In order to consider the crossing orientation of the human body blockage, the angle α is used to represent the angle between the LOS and the normal vector to the rectangular plate.

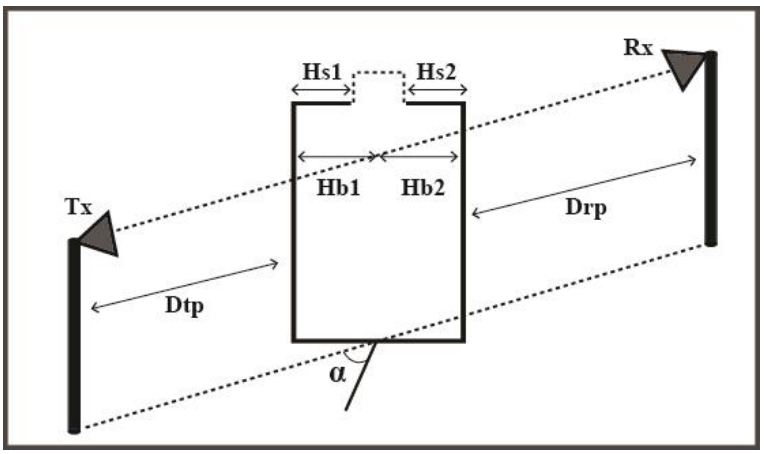

Figure 3.1 Geometric model representing the human body

It should be noted that the diffraction components from the edges of H_{s1} and H_{s2} (representing the shoulders of the human model) should be considered for antenna heights being higher than the chest of the human body, as they are contained within the first Fresnel Zone. Therefore, two methods can be used in calculating the human body shadowing gain. For low antenna heights being less than the chest level of the human the two vertical edge-diffractions are most dominated. On the other hand, multiple-edge diffractions taking into account shoulders' diffractions is used for higher antenna heights.

The Fresnel diffraction method is used to describe the mentioned diffraction effect. The diffraction gain is expressed as [35]

$$G_l = \frac{1+j}{2}\left\{\left(\frac{1}{2} - C(v)\right) - j\left(\frac{1}{2} - S(v)\right)\right\} \tag{3.1}$$

where G_l is the Fresnel integral and the numerical approximation of the Fresnel integration for C(v) and S(v) are defined as

$$C(v) = \int_0^v \cos\left(\frac{\pi v^2}{2}\right)\, dv \tag{3.2}$$

$$S(v) = \int_0^v \sin\left(\frac{\pi v^2}{2}\right)\, dv \tag{3.3}$$

where v is the Fresnel-kirchhoff diffraction parameter

$$v_{(\theta)} = \theta\sqrt{\frac{2}{\lambda}\frac{d_T d_R}{d_T + d_R}} \tag{3.4}$$

where θ is the diffraction angle and is expressed as

$$\theta_{(h)} = \tan^{-1}\left(\frac{h}{d_T}\right) + \tan^{-1}\left(\frac{h}{d_R}\right) \tag{3.5}$$

when the crossing orientation angle α is taken into account, then the effective height h and distances dT, and dR can be calculated as

$$h = h' \cos \alpha \tag{3.6}$$

$$d_T = d_{tp} \pm h' \sin \alpha \tag{3.7}$$

$$d_R = d_{rp} \pm h' \sin \alpha \tag{3.8}$$

where h' denote H_{b1}, H_{b2}, H_{s1} and H_{s2}.

In lateral crossing shown in Fig. 3.2a, the crossing orientation angle α is equal to 0°, whereas for frontal crossing (Fig. 3.2b) the angle α is defined to 90°. In the frontal crossing case the thickness of the human body will have an impact on the effective height. As a result, the distances d_T, d_R and the effective height h and the are calculated as

$$d_T = d_{tp} \pm H_b \tag{3.9}$$

$$d_R = d_{rp} \pm H_b \tag{3.10}$$

$$h = max(h' \cos \alpha , W_T) \tag{3.11}$$

where the thickness of human body is defined as W_T. Thus, the total human body shadowing (HBS) gain is expressed as

$$G_{total} = \sum_{l=1}^{n} G_l \tag{3.12}$$

where n is the total number of diffraction components taken into account.

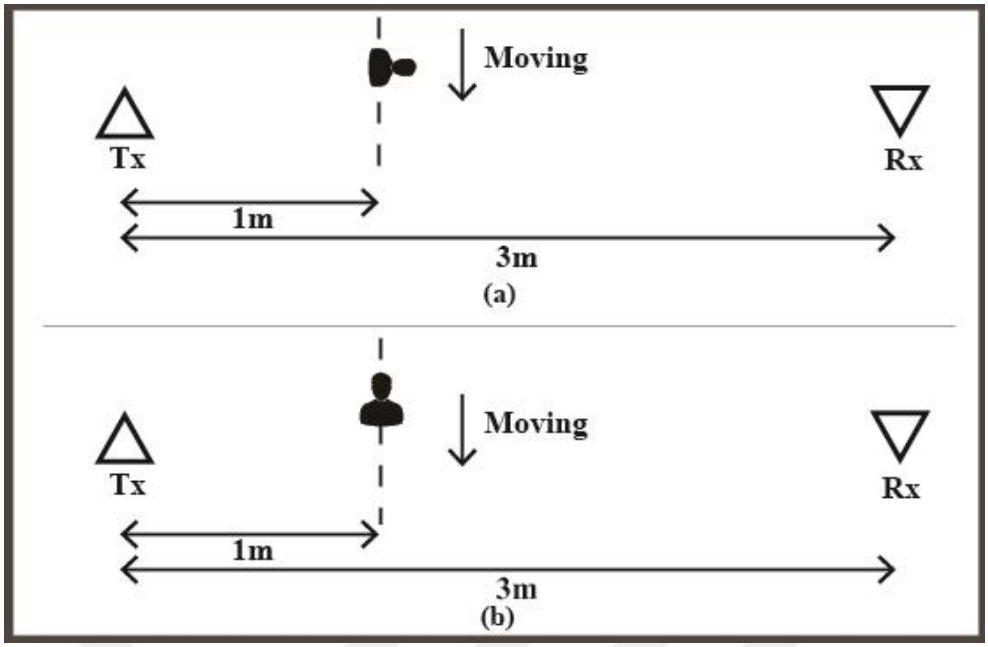

Figure 3.2 Example of lateral and frontal crossing of the LOS. (a) Lateral crossing. (b) Frontal crossing.

3.2 Human Blockage Measurements

In the measurement scenario shown in Fig. 3.2, the Tx and Rx antennas were separated by a distance of 3m. Three different Tx heights were used which are 1m, 1.3m and 1.6m. Two different LOS crossing orientations were investigated, both lateral and frontal crossing. Three different human models having various body dimensions were used in the measurements. The human models' dimensions are given in Table. 3.1. The human subjects crossed the LOS path at 1m away from the Tx antenna, which is at the far-field region for the antennas at 28GHz.

Table 3.1 Human Models Dimensions

	Height	**Width (Hb)**	**Thickness (W_T)**	**Shoulder (Hs)**
Model 1	188 cm	48 cm	22 cm	16 cm
Model 2	173 cm	44 cm	22 cm	14 cm
Model 3	166 cm	40 cm	24 cm	12 cm

In doing the measurements, the human model was moving from -1m to 1 m crossing the LOS path (where the position point at 0m refers to the direct path between the Tx

and Rx) with increment of 0.1m, and a total of 21data points were measured. Due to the system limitation, continuous time measurements could not be done; therefore, the measurement had to be done with the human model moving step by step. The received power was measured for each step as the person moves toward crossing the LOS. In the measurements, the data was recorded at each position over several time periods and over several days, then the mean value was calculated to provide accuracy to the reported results and to prevent any randomness in the measurements. Also, the received power was measured when the Tx and Rx were placed in free space where no human blockage is present in order to evaluate the effect of the human blockage precisely.

In this study, we evaluated the human body size, crossing orientation and the Tx height effect on human blockage loss. Table. 3.2 represent the experimental measurements of the 3 different human models in terms of blockage loss, highlighting the effect of both transmitter height and crossing orientation. When observing the same human model, no significant difference is observed for Tx=1m and Tx=1.3m. However, the height of the model plays an important role when Tx=1.6m; therefore, human model 1(1.88m height) has a considerable effect when the Tx height is at 1.6m. Along with the human height, the side width plays an important role for Tx=1.6m (Difference can reach up to 16dB in frontal crossing case and 18dB in lateral crossing). No huge difference is observed when comparing the human models in case of Tx=1m and Tx=1.3m, in frontal crossing case. This is mainly due to the reason that all human models have got almost the same body thickness within range of 22-24cm.

Table 3.2 Blockage loss measurements

	Tx=1m		**Tx=1.3m**		**Tx=1.6m**	
	Frontal crossing	**Lateral crossing**	**Frontal crossing**	**Lateral crossing**	**Frontal crossing**	**Lateral crossing**
Model 1	13 dB	21 dB	14 dB	20 dB	20 dB	24 dB
Model 2	14 dB	26 dB	13 dB	21 dB	7 dB	13 dB
Model 3	14 dB	23 dB	12 dB	21 dB	4 dB	6 dB

When analysing the experimental measurements in terms of crossing orientation, it was found that the blockage loss and fading distance is always higher in lateral crossing when compared to frontal crossing. The difference is less significant when

Tx=1.6m. The difference of the blockage loss and fading distance between lateral crossing and frontal crossing is given in Table. 3.3. For Tx height of 1.3m, the difference can reach up to 13dB in blockage loss. This difference reduces to range of 2-6 dB when the Tx height is increased to 1.6m. The fading distance increases by 10-20cm in lateral crossing orientation in most of the considered scenarios (considering different human models and different transmitter heights).

Table 3.3 Difference between lateral crossing and frontal crossing in terms of blockage loss and fading distance

	Blockage loss (dB) and Fading Distance (cm)					
	Tx=1m		**Tx=1.3m**		**Tx=1.6m**	
Model 1	8 dB	10 cm	6 dB	20 cm	4 dB	20 cm
Model 2	6 dB	20 cm	13 dB	10 cm	6 dB	20 cm
Model 3	9 dB	20 cm	9 dB	20 cm	2 dB	-

The human blockage model given in the previous section based on the Fresnel diffraction method is compared with the experimental measurements, as well as the GTD model. Human blockage models based on GTD [36] had been popularly considered in the literature for sub-6GHz frequency bands as in [37, 38] and in mm-Wave frequency bands as in [14, 16, 19].

The human body shadowing gain of human Model 2 for Tx height of 1m considering both lateral and frontal crossing is shown in Fig. 3.3. It can be seen that the human blockage model based on Fresnel diffraction method fits well the measurements, especially for the case of lateral crossing (Fig. 3.3b) in which the GTD model significantly underestimates the HBS gain. This is mainly due to the reason that the GTD model is based on representing the human body as a cylindrical shape which is independent of the orientation of the human body. Furthermore, the GTD based model cannot be used in scenarios that use different antenna heights as the GTD model is able to analyse the scattering problem in 2-D space only. When the scattering problem is extended to 3-D the closed form solutions of the scattering field do not exist, as the case in investigating the antenna height effect on human blockage loss. Therefore, the given human blockage model based on Fresnel diffraction overcomes those mentioned shortcoming by taking into consideration both the orientation of the human body, as well as considering its finite height. Table. 3.4 represent the difference between the

Fresnel diffraction human blockage model and the performed experimental measurements considering all 3 human models and both lateral and frontal crossing for Tx height of 1m and 1.3m.

Table 3.4 Difference between the given theoretical model and measurements

	Frontal crossing	**Lateral crossing**
Model 1	4 dB	4 dB
Model 2	3 dB	2 dB
Model 3	4 dB	3 dB

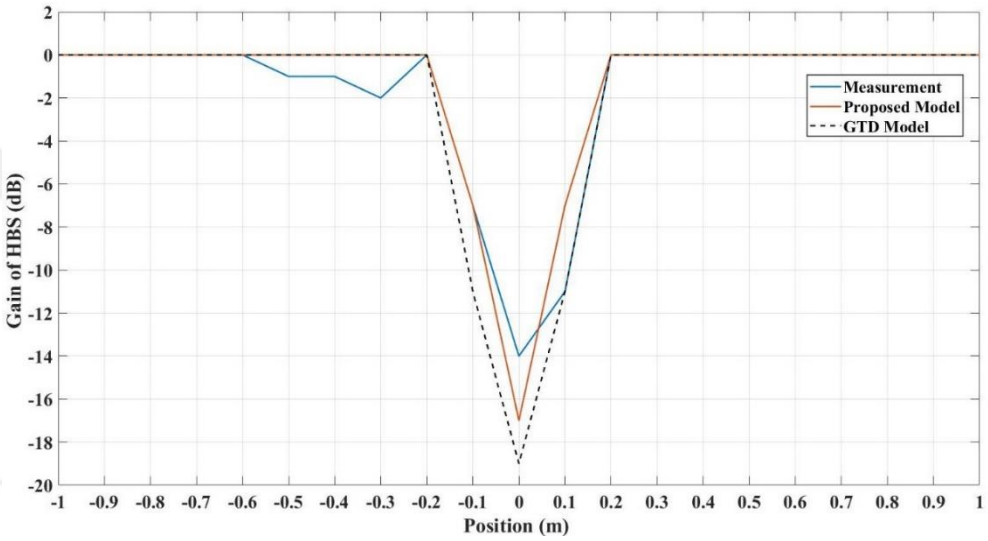

(a)

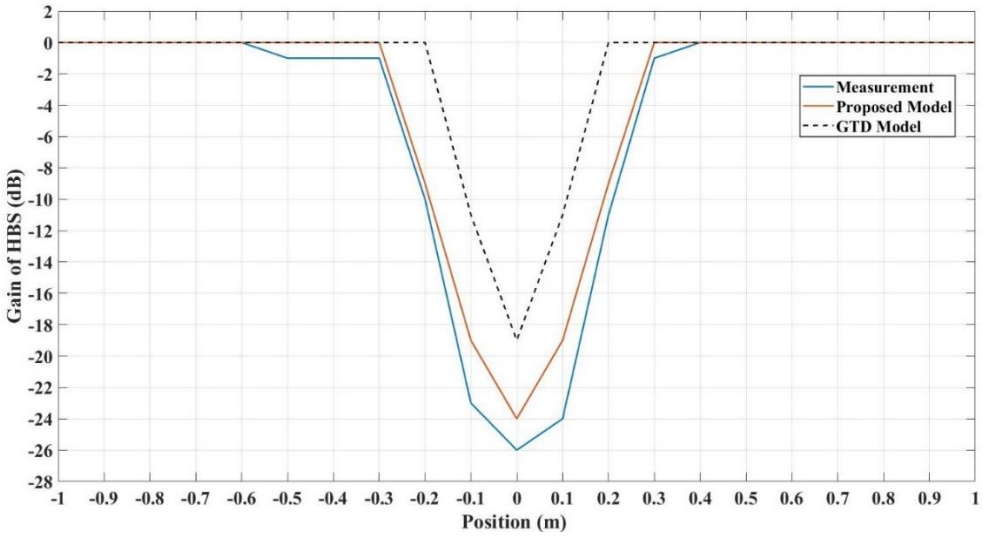

(b)

Figure 3.3 Human body shadowing gain of human Model 2 for Tx height of 1m. (a) Frontal crossing. (b) Lateral crossing.

In the case when the Tx height is 1m and 1.3m only the diffractions from the side edges of the human model are considered. However, when the height of the Tx is increased to 1.6m the diffractions from the shoulders should be taken into account especially in the case of tall human models as human model 1 used in this study. Taking those diffraction components into consideration, the accuracy of the Fresnel diffraction human blockage model enhances significantly. The HBS gain of human Model 1 for Tx height of 1.6m considering frontal crossing is shown in Fig. 3.4. It can be seen that the human blockage model based on Fresnel diffraction method fits well the measurements with difference around 1-2dB only.

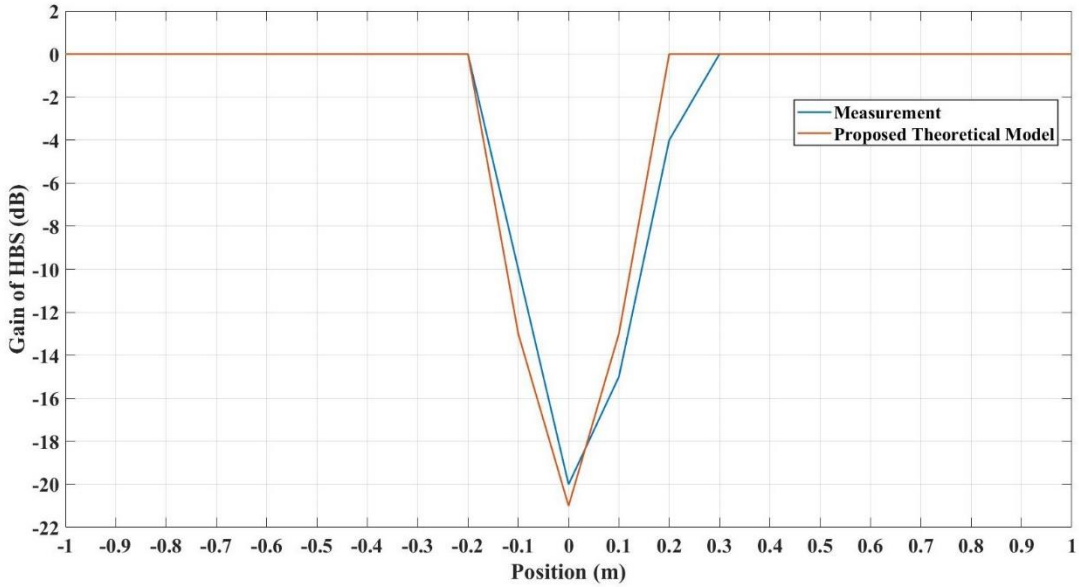

Figure 3.4 Human body shadowing gain of human Model 1 at Tx height of 1.6m for frontal crossing case.

From the reported results it can be seen clearly that the human blockage model based on Fresnel diffraction can accurately estimate the human blockage effect at 28GHz taking into account different human body dimensions, crossing orientation and antenna height.

CHAPTER 4

SMALL-SCALE FADING STATISTICS

4.1 Measurement Setup

The communication system used in this experimental study consists of a signal generator (Agilent E8244A), a spectrum analyzer (Agilent E4448A), two identical horn antennas (PE9850/2F-20) having a gain of 20 dBi with 16.7° vertical and 18.3° horizontal half-power beamwidth (HPBW), and low loss cables were used to make the connections. Based on the experimental scenario setup, three stands were used (1m, 1.3m and 1.6m) for placing the antennas on. The link between the antennas was aligned using a laser pointer. The separation between the transmitter and the receiver was 4.7m.

The measurements were performed in a typical indoor office environment (9.40×5.15m) at the school of Engineering, Atilim University. The office is a typical working environment having several chairs, desks with computers, as well as cabinets. The floor plan of the environment is given in Fig. 4.1. The distances from the communication link to both sides of the wall are denoted by L1=2.65m and L2 =2.5m. The transmitter is placed in front of a wall (at L3 =0.8m), and behind the receiver there are wooden cabinets of 1.92m height (at L4 =3.9m behind the receiver). In the experiment, the link is set about the mid of the office, in which various human activities are observed during several time periods of working hours. In all of the measurements, a human blockage is present at 3m away from the transmitter, which is completely blocking the LOS propagation link. As the fluctuation of the received signal at mm-Wave frequency bands due to human blockage movements is greater in NLOS situations when compared to LOS scenarios, this makes investigating the NLOS scenarios a research interest.

Three different combinations of transmitter's antenna height were used (Tx=1m, Tx=1.3, and Tx=1.6m). The receiver's height was 1m for all scenarios, and the positions of both the transmitter and receiver remained the same. The antenna heights combinations used in the experiments were determined based on real life scenarios for device-to-device communication. Three and six human activities were investigated for each of the mentioned antenna heights. Human activities refer to the total number of persons present in the office at the time of the measurements. The measurements were recorded in various time periods over several days, in which a video-camera recorded the scene. The video records were used to analysis the human blockage movements around the propagation link.

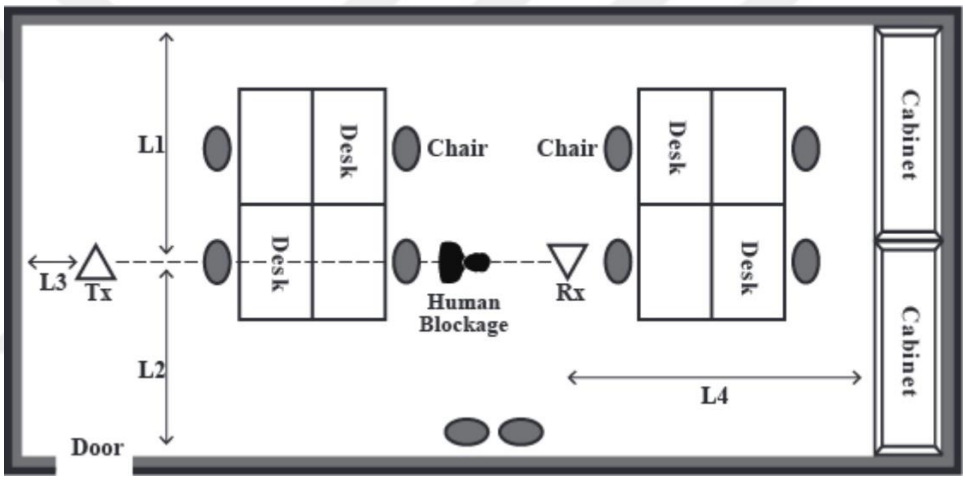

Figure 4.1 Floor plan of the office environment.

The human activties within the office can be described in terms of the following paths based on the labled positions in Fig. 4.2:

- Direct path from the door (position 1) to any of the offices (position 2-5) and vice versa.
- Movement between the desks of the working colleagues (position 2-5).
- Direct path from the offices (position 2-4) to the coffee machine area (position 6) and vice versa.
- Movement from the desks (position 2-4) toward the cabinets (position 7).

These movements described above were defined as stochastic processes where the experimental had no control of the human activity inorder to describe real life indoor scenraios.

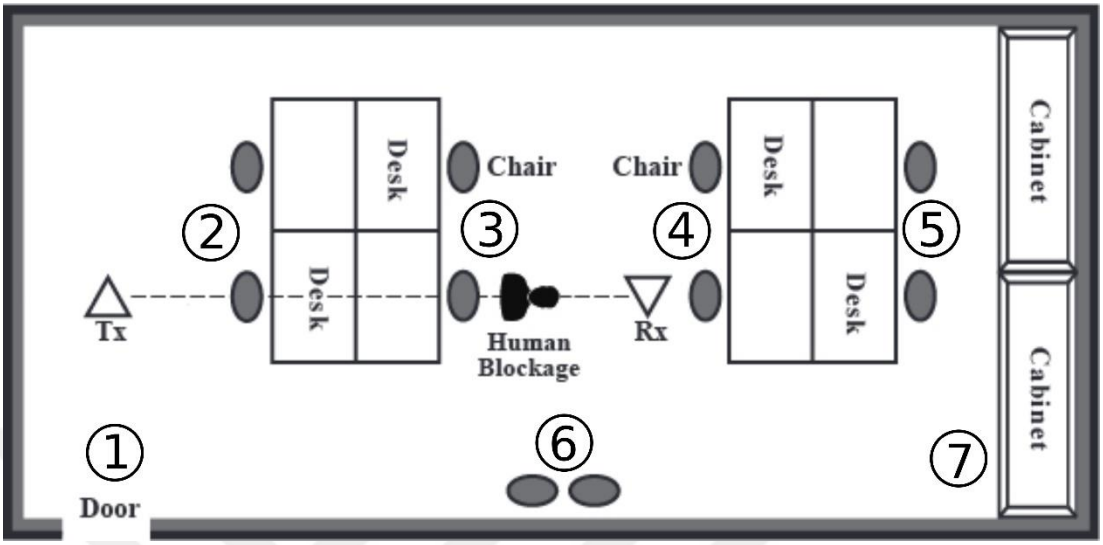

Figure 4.2 Human activity paths within the office environment based on the labeled positions 1 to 7.

The experiments were performed in order to investigate the effect of human blockage movement on the received signal at 28GHz considering both increase in number of human activity and the transmitter antenna height. In this study, three propagation characteristics are considered. These investigated characteristics are the human blockage shadowing duration, human blockage maximum temporal fading, and the overall path loss due to human blockage movements.

The ratio of the transmitted power to the received one is defined as the attenuation A(t). It is observed that the attenuation strongly increases when the link is blocked by humans' activity. Those sharp attenuations are defined as the human blockage shadowing event (SE). The attenuation caused by three persons' activity within the

office environment at antenna heights of 1m is given in Fig. 4.3. When the attenuation is greater than a defined threshold the SE is detected. In this study, a threshold level of 20dB is used, which was determined experimentally as it was observed that different human models having various heights and widths can be detected for a threshold level of 20dB higher than a reference attenuation level (A_{ref}). The A_{ref} is the amount of attenuation when there is nobody present in the office.

The attenuation caused by the human blockage can be characterized in terms of both duration and amplitude as given in Fig. 4.4. The instant that the threshold level is crossed with a positive slope (T_B), the beginning of the SE is defined and the end of the SE (T_E) is represented by the crossing of the threshold level with a negative slope. By following this method, each SE duration (D_S) is given as

$$D_S = T_E - T_B \tag{4.1}$$

The temporal fading F(t) caused by the SE is defined as the amount of attenuation beyond the threshold level

$$F(t) = A(t) - A\text{threshold} \tag{4.2}$$

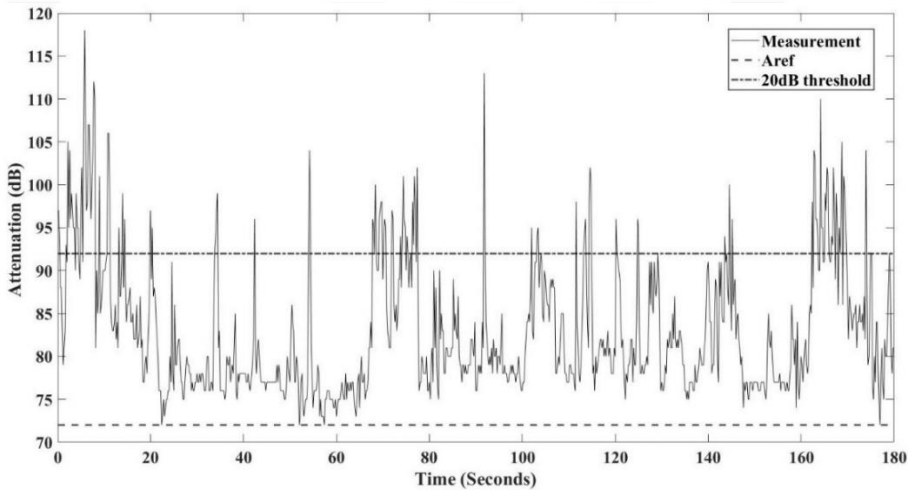

Figure 4.3 Attenuation caused by three persons' activity at Tx=1m is given.

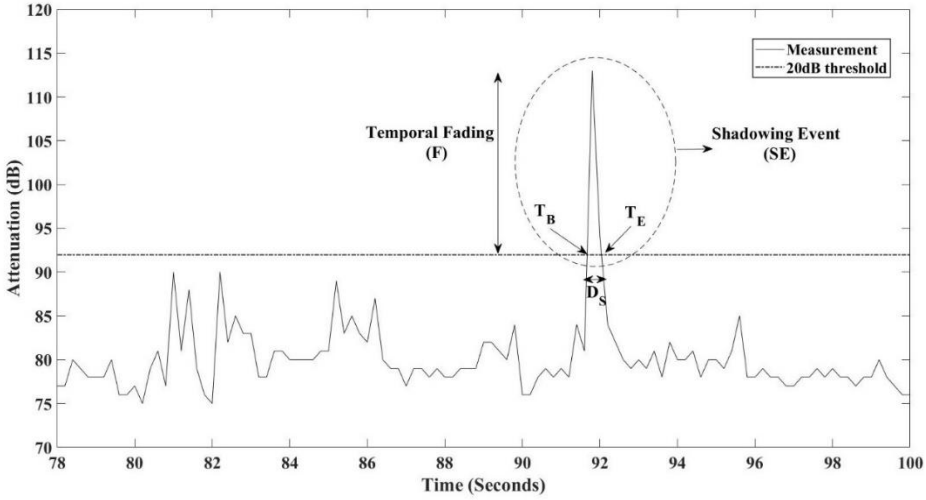

Figure 4.4 Shadowing event characterization.

4.2 Measurement results and empirical models

In analysing the measured data two parameters were taken into consideration, which are the number of human activities and the transmitter antenna height. The data files were split into several parts based on these two parameters, and the human blockage SE duration, the human blockage maximum temporal fading, as well as the overall path loss were analysed and discussed accordingly.

The human blockage SE Cumulative Distribution Function (CDF) of a three persons' activity for both antenna heights being at 1m is shown in Fig. 4.5a. Similarly, the six persons' activity CDF for the same antenna heights is given in Fig. 4.5b. The median and the 95th percentile of the SE duration considering three and six human activity for all antenna heights (Tx=1m, 1.3m, and 1.6m) are summarized below:

• For the activities of three humans: the median was 0.2s for all transmitter antenna heights, while for the 95th percentile was 1s for Tx=1m, 1.4s for Tx= 1.3m, and 1.2s for Tx=1.6m.

• For the activities of six humans: the median was found to be the same for Tx=1m, and 1.3m, having a duration of 0.4s. For Tx=1.6m, the median of the SE duration was the same as the three humans' activity of 0.2s. The 95th percentile for Tx=1m was 2.2s, for Tx= 1.3m it was 3.4s, and 1.2s for Tx=1.6m.

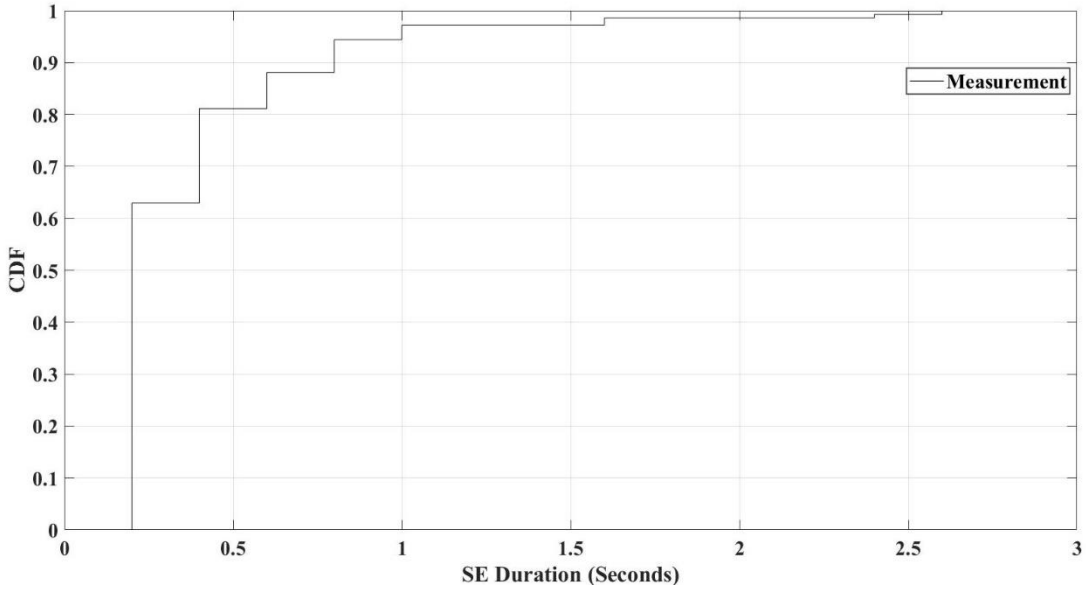

(a)

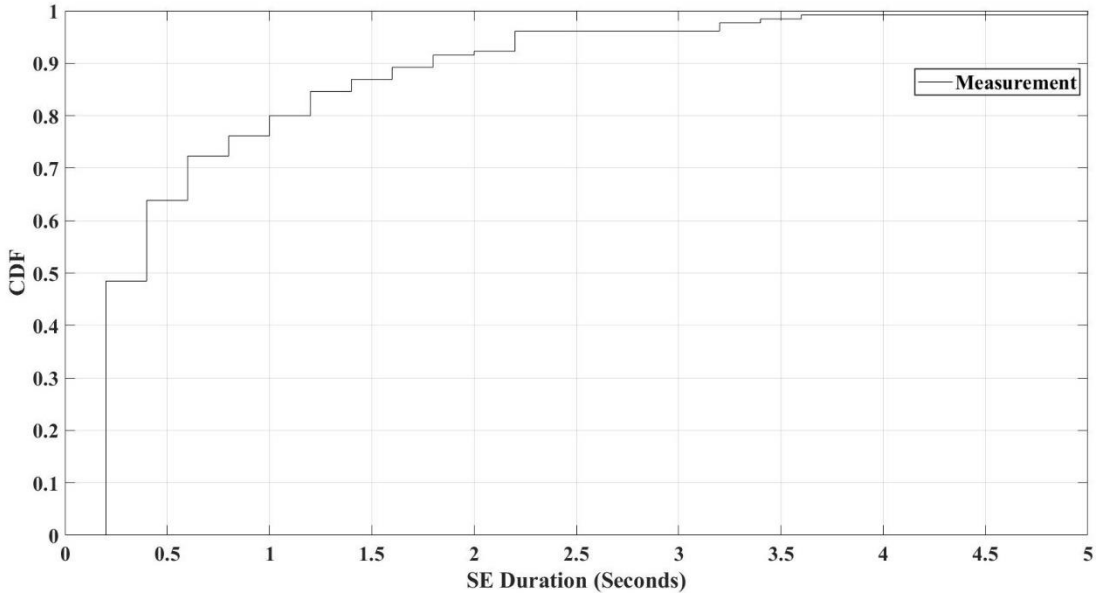

(b)

Figure 4.5 CDF of the SE duration for Tx=1m. (a) 3 humans' activity. (b) 6 humans' activity.

The human blockage SE duration median values, the 90th and 95th percentiles of three humans' activities and six human's activity are given in Table. 4.1 and Table. 4.2, respectively. The total number of the recorded SEs are given in Table. 4.1 and Table. 4.2 to provide an overview of the available data sample.

Table 4.1 Statistics of SE duration for 3 people activity

Antennas Height	**SE Duration (s)**			
	Number of SE	***Median Value***	***90th Percentile***	***95th Percentile***
Tx= 1m and Rx=1m	143	0.2	0.8	1
Tx= 1.3m and Rx=1m	126	0.2	1	1.4
Tx= 1.6m and Rx=1m	95	0.2	0.8	1.2

Table 4.2 Statistics of SE duration for 6 people activity

Antennas Height	**SE Duration (s)**			
	Number of SE	***Median Value***	***90th Percentile***	***95th Percentile***
Tx= 1m and Rx=1m	130	0.4	1.8	2.2
Tx= 1.3m and Rx=1m	151	0.4	2.2	3.4
Tx= 1.6m and Rx=1m	117	0.2	0.8	1.2

From the given results, it is seen that increasing the antenna height does not affect the median human blockage SE duration, especially for three humans' activities. The effect of increasing the transmitter antenna height is clearly seen when analysing the 95th percentile, which represent the worst case scenarios of the human blockage SE duration. In such cases, it was observed that the transmitter heights of 1.3m had the longest duration. This is mainly due to the blockage of the signal by the chest/abdomen sections of the human body.

For six humans' activity when the transmitter is at 1.6m, the worst case SE duration due to human blockage was considerably lower. Also, it can be observed that for 6 persons' activity when the Tx=1.6m, the SE duration is considerably lower for the 90th and 95th percentile when compared to the other antenna height combinations. As several human blockages' height being in range about this height of the transmitter or even less, the blockage effect on the propagation link was not significant.

The fast variations of the human blockage SE duration median value increases by 200ms when the human activity is increased from three to six persons, for both transmitter heights 1m and 1.3m, and for the worst case scenarios (95th percentile) this increase can be up to 2s when transmitter height is 1.3m.

The Probability Density Function (PDF) of the human blockage SE duration for three and six humans' activity is given in Fig. 4.6, Fig.4.7 and Fig. 4.8, for Tx=1m, Tx=1.3m, and Tx=1.6m, respectively. It was found that the duration of the SE characteristic follows an exponential distribution. The dashed line in Fig. 4.6, Fig. 4.7 and Fig. 4.8, represent the estimated exponential curve as a function of the SE duration, x, (in seconds)

$$f(x) = \frac{1}{\mu}\exp\left(-\frac{x}{\mu}\right) \tag{4.3}$$

where μ is the mean of the exponential distribution.

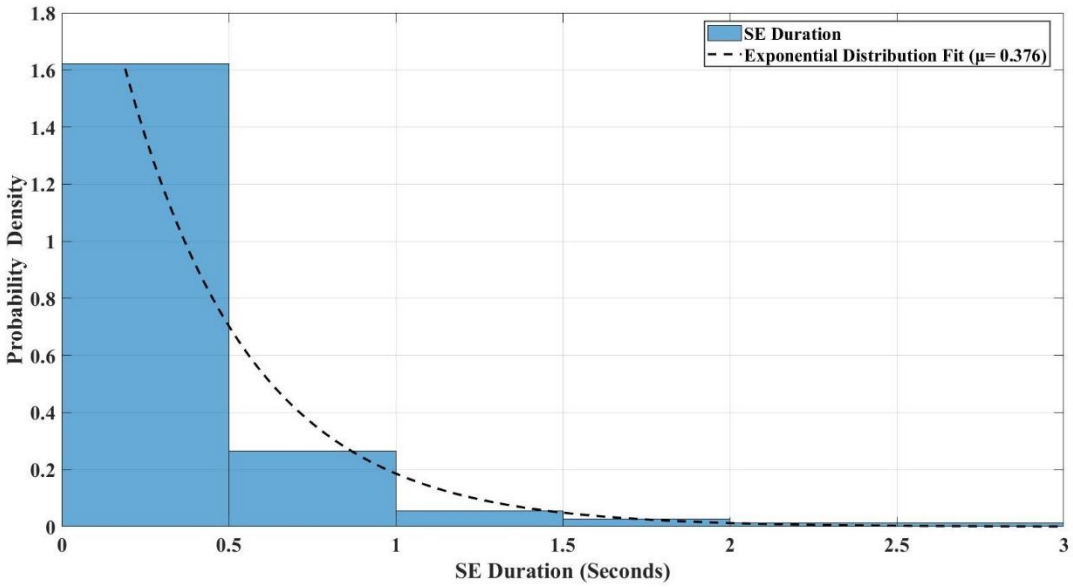

(a)

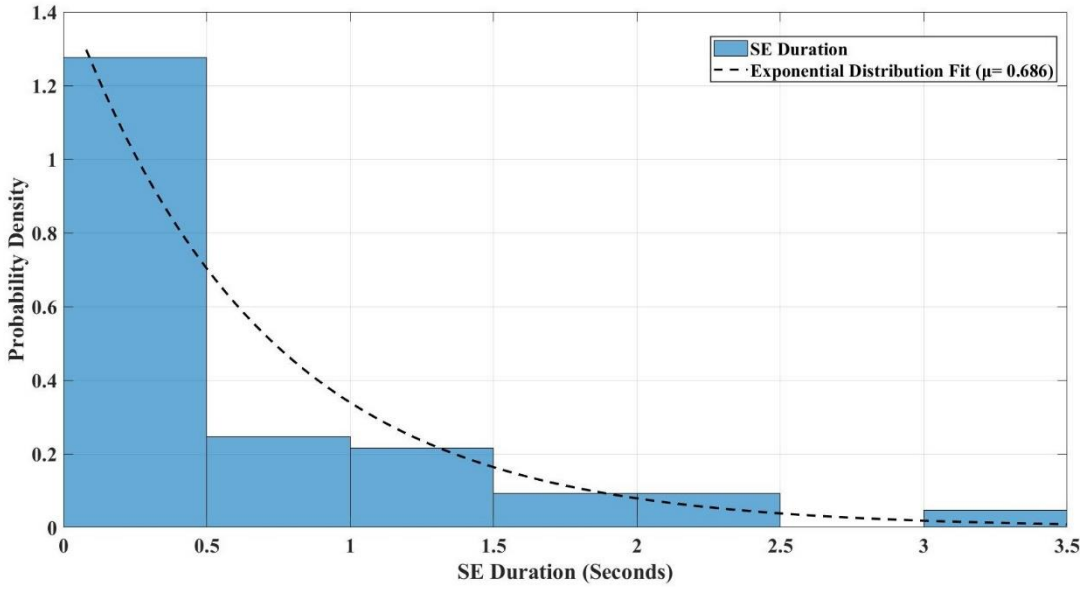

(b)

Figure 4.6 PDF of the SE duration for Tx=1m. (a) 3 humans' activity. (b) 6 humans' activity.

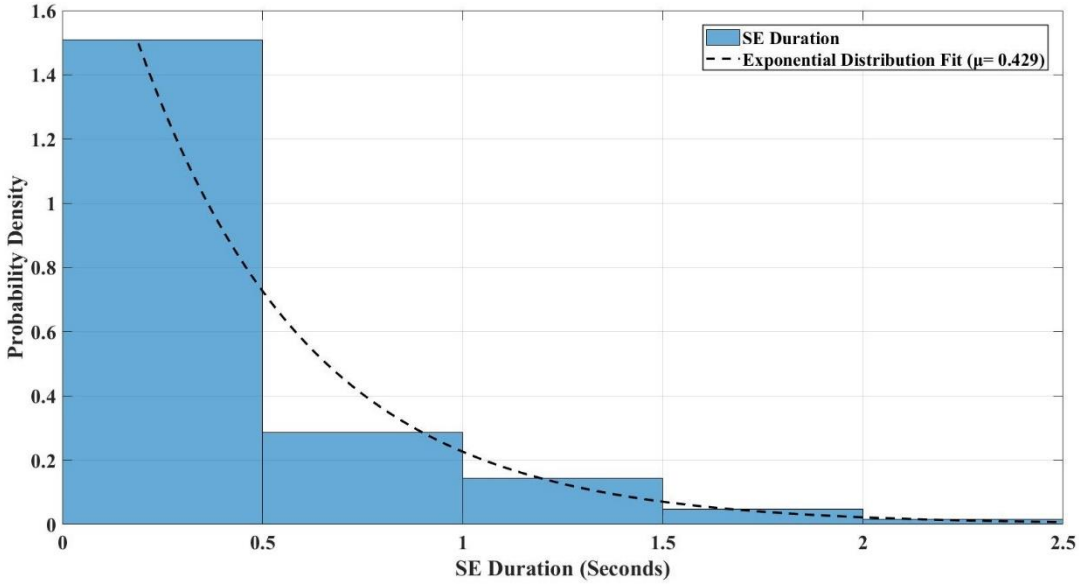

(a)

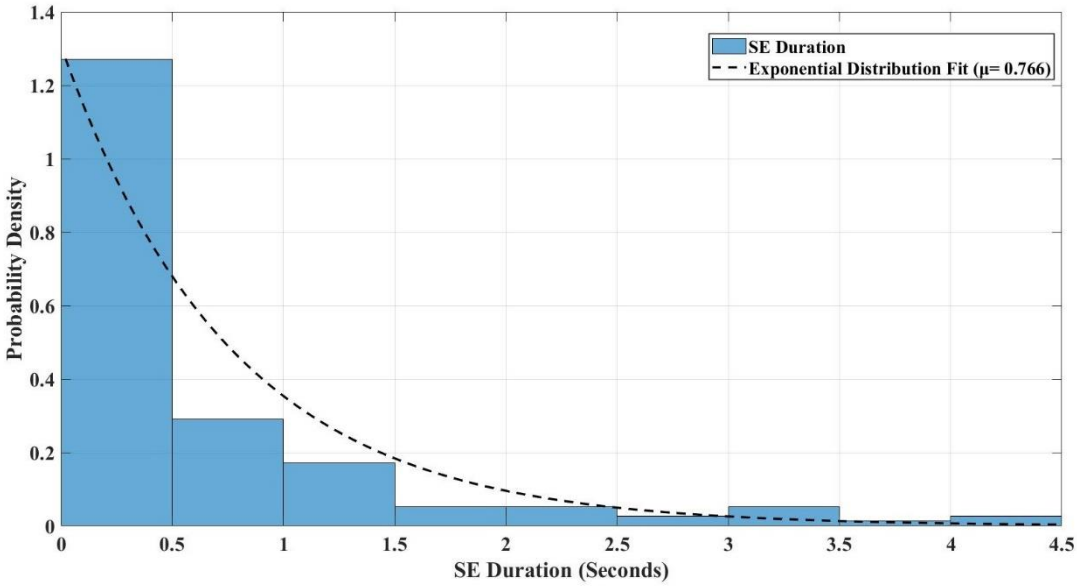

(b)

Figure 4.7 PDF of the SE duration for Tx=1.3m. (a) 3 humans' activity. (b) 6 humans' activity.

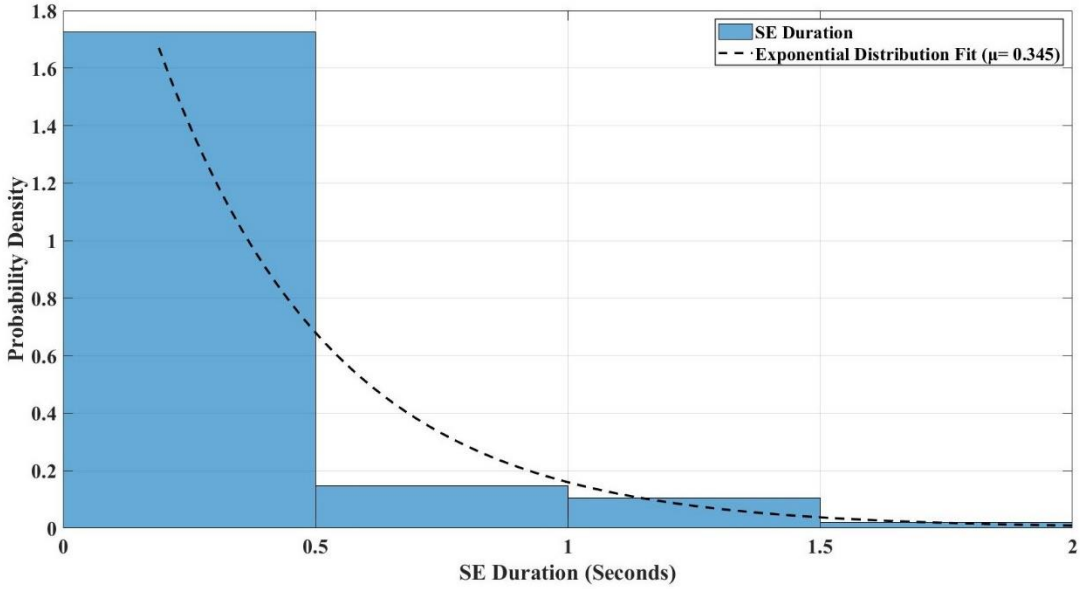

(a)

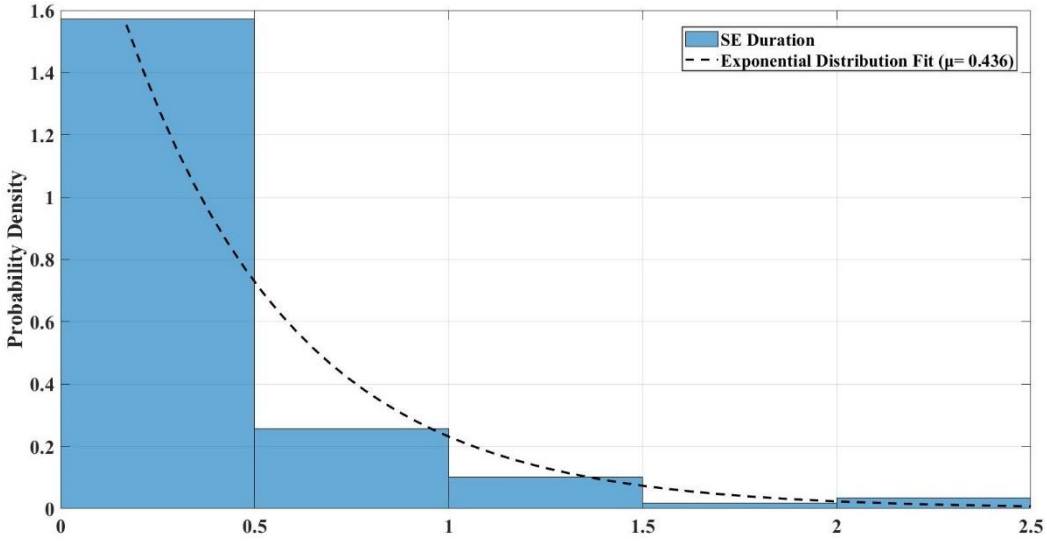

(b)

Figure 4.8 PDF of the SE duration for Tx=1.6m. (a) 3 humans' activity. (b) 6 humans' activity.

The following key figures summarize the mean human blockage SE duration regarding all antenna heights and human activities based on the proposed empirical model:

• For the activities of three humans: increasing the transmitter height from 1m to 1.3m, increases the SE duration mean value from 376ms to 429ms, whereas for transmitter height of 1.6m, the mean is found to be the lowest with 345ms.

• For the activities of six humans: increasing the transmitter height from 1m to 1.3m, increases the SE duration mean value from 686ms to 766ms, whereas for transmitter height of 1.6m, the mean is found to be the lowest with 436ms.
• Comparison of the humans' activities between three and six persons: for transmitter height of 1m, increase in people increases the mean by 310ms, for 1.3m the increase in mean is 337ms, and for 1.6m the increase in mean is 91ms.

The maximum human blockage temporal fading is given in Table. 4.3. It was observed that the blockage fading may vary in range from 17dB to 30dB based on the number of humans' activity within the office and the height of the transmitter. The increase in the number of human blockages does not affect the fading significantly when the transmitter is at 1m and 1.6m height; however, this increase has a great effect when the height is 1.3m with a difference of 10dB, comparing three and six people activities. This is primarily due to the reason that the human blockages are completely blocking the signal at this transmitter height (1.3m), as the cross section of the chest/abdomen is wider than the beam-width of the antenna there were no diffracted rays presented. When the transmitter is at 1m and 1.6m height, this occasion is not the same as the signals were diffracted from the shoulders of the human body, as well as from the sides of the legs.

Table 4.3 Statistics of the maximum temporal fading for 3 and 6 people activity

Antennas Height	**SE Temporal Fading (dB)**	
	3 people activity	**6 people activity**
Tx= 1m and Rx=1m	26	28
Tx= 1.3m and Rx=1m	20	30
Tx= 1.6m and Rx=1m	19	17

In order to investigate the path loss taking into account the human blockage movements, the path loss values are normalized according to the path loss measurements when there are no humans present within the office environment. Table. 4.4 and Table. 4.5 illustrate the statistics of the normalized path loss for mean, median,

the 90th and the 95th percentiles of both three and six humans' activities, considering all antenna heights combinations.

Table 4.4 Statistics of the normalized path loss for 3 people activity

Antennas Height	**Normalized path loss (dB)**			
	Mean Value	***Median Value***	***90th Percentile***	***95th Percentile***
Tx= 1m and Rx=1m	13	11	23	27
Tx= 1.3m and Rx=1m	13	11	23	27
Tx= 1.6m and Rx=1m	12	11	20	24

Table 4.5 Statistics of the normalized path loss for 6 people activity

Antennas Height	**Normalized path loss (dB)**			
	Mean Value	***Median Value***	***90th Percentile***	***95th Percentile***
Tx= 1m and Rx=1m	15	13	28	31
Tx= 1.3m and Rx=1m	18	17	30	35
Tx= 1.6m and Rx=1m	12	10	23	27

It was found that the normalized path loss due to human blockage movements follows a lognormal distribution. The path loss due to three and six humans' activity is given in Fig. 4.9, Fig.4.10 and Fig. 4.11, for Tx=1m, Tx=1.3m, and Tx=1.6m, respectively. The PDF and CDF of the lognormal distribution fit are given as

$$f(x;\ \mu,\sigma) = \frac{1}{x\sigma\sqrt{2\pi}} \exp\left(-\frac{(lnx-\mu)^2}{2\sigma^2}\right) \tag{4.4}$$

$$\mathrm{F}(x;\ \mu,\sigma) = \frac{1}{2} + \frac{1}{2}\ \mathrm{erf}\left[-\frac{(lnx-\mu)}{\sqrt{2}\,\sigma}\right] \tag{4.5}$$

where μ is the mean, σ is the standard deviation, and erf is the Gauss error function.

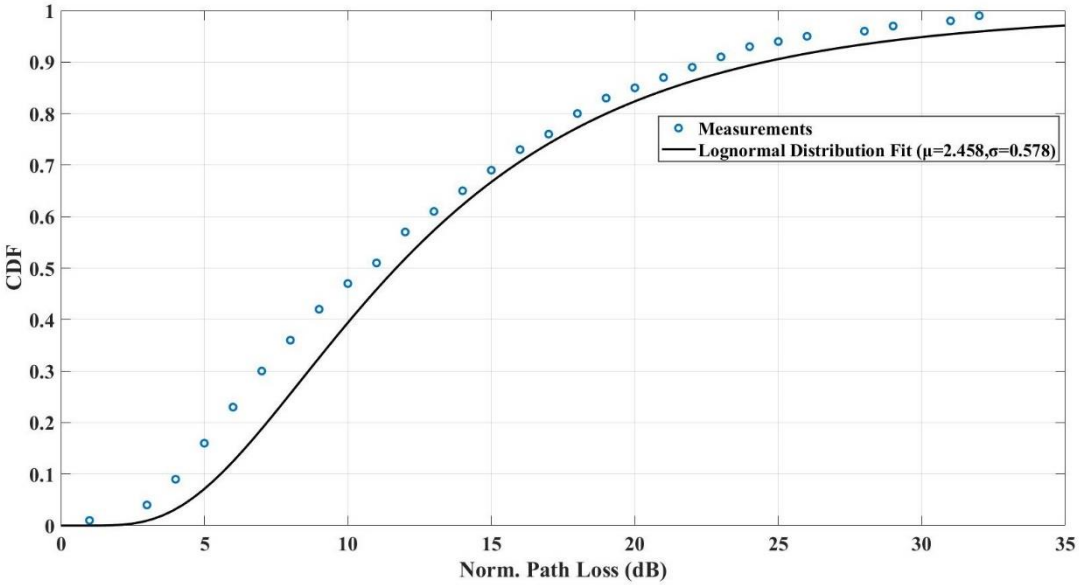

(a)

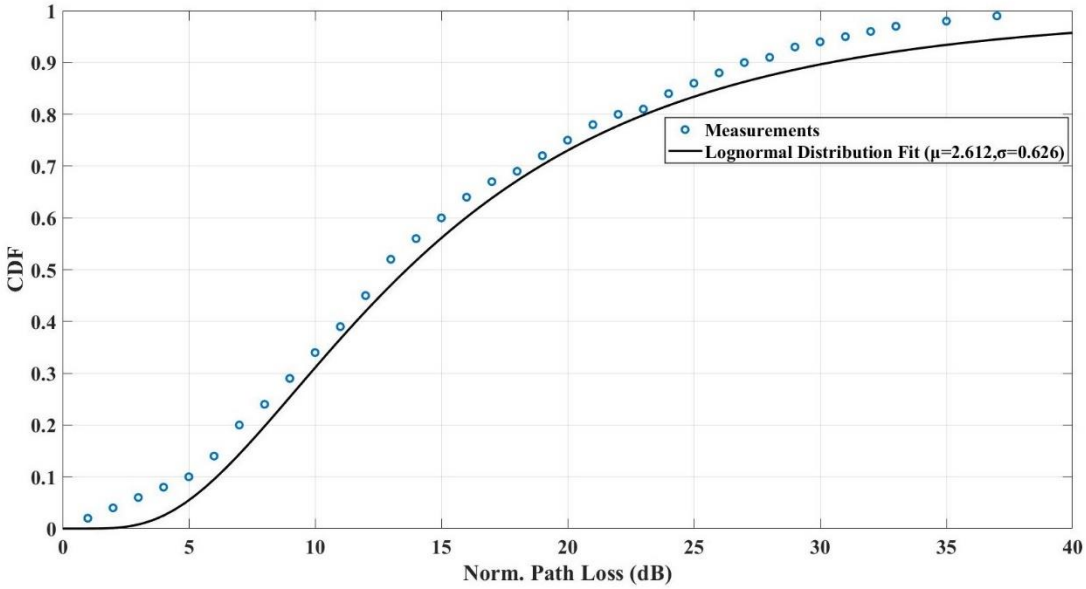

(b)

Figure 4.9 CDF of the normalized path loss for Tx=1m (a) 3 humans' activity. (b) 6 humans' activity.

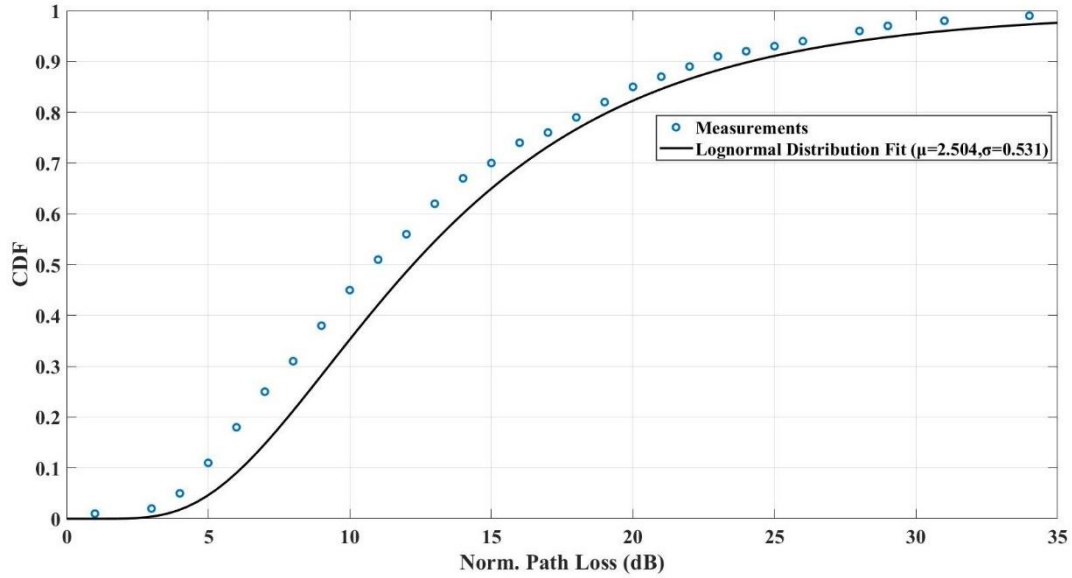

(a)

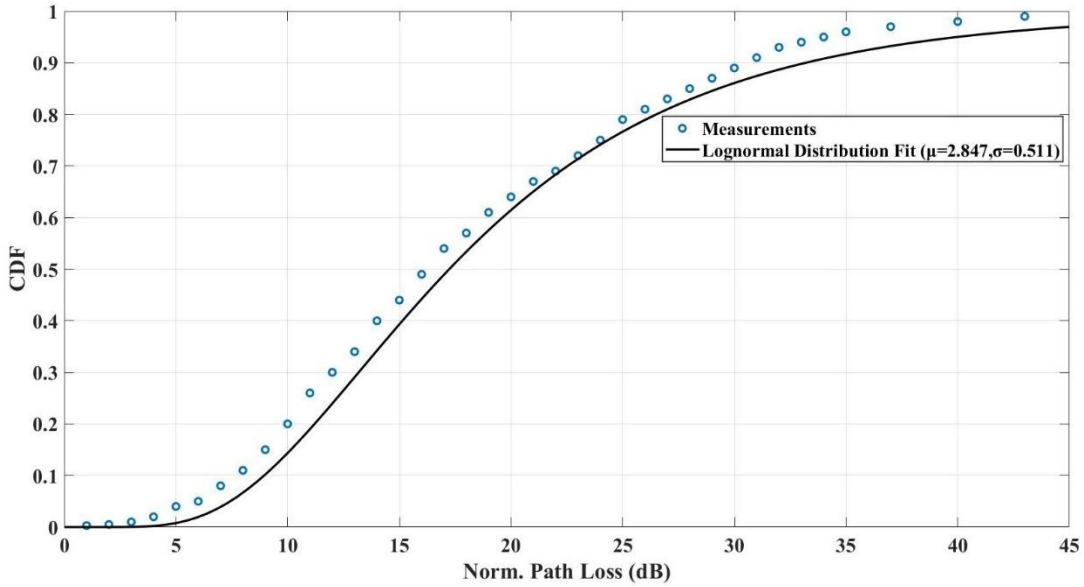

(b)

Figure 4.10 CDF of the normalized path loss for Tx=1.3m. (a) 3 humans' activity. (b) 6 humans' activity.

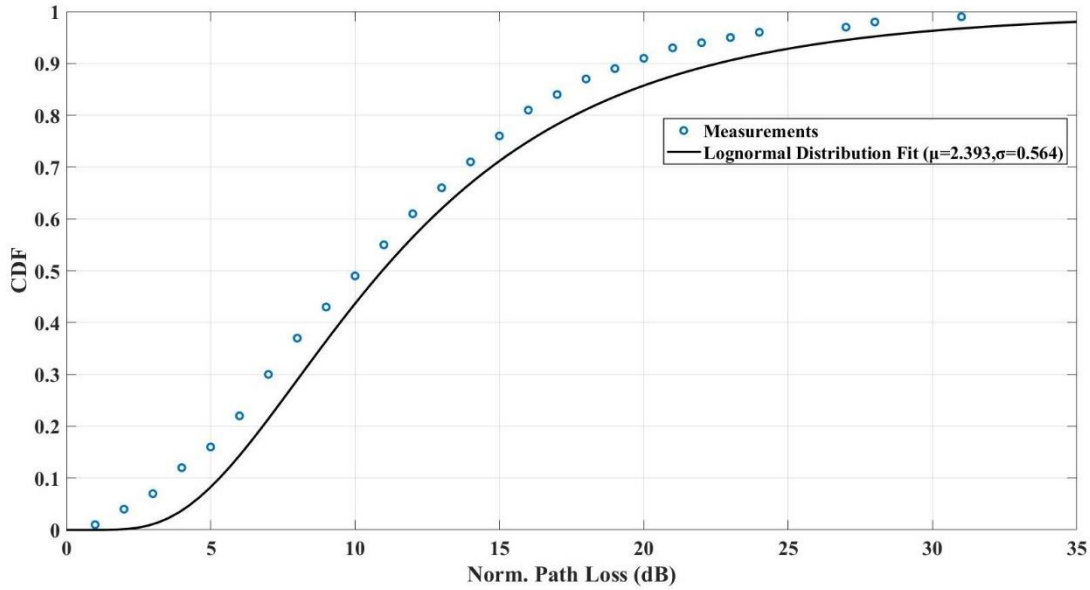

(a)

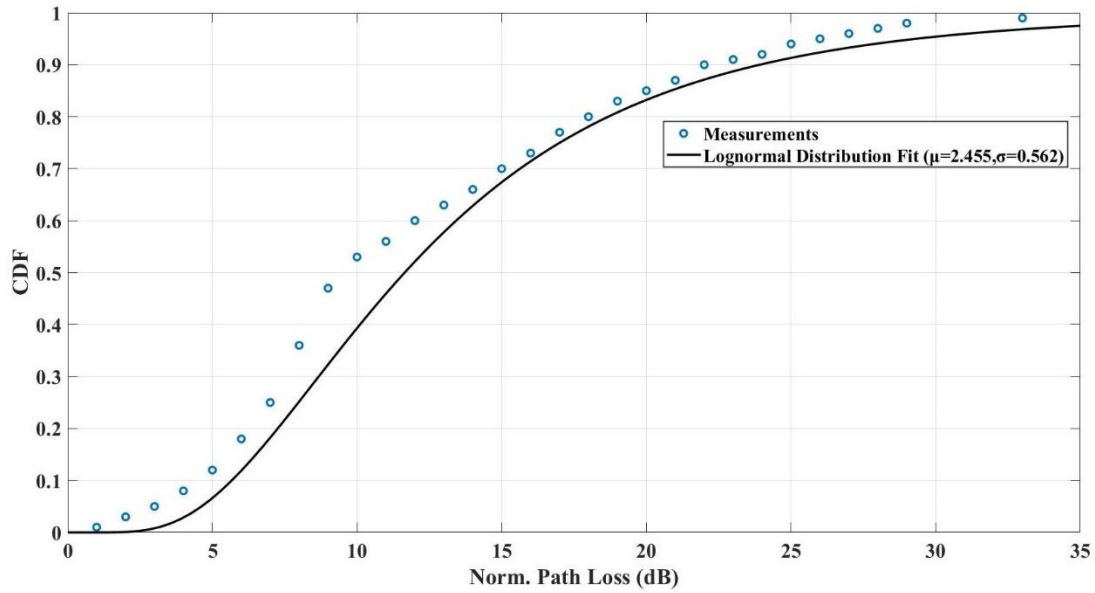

(b)

Figure 4.11 CDF of the normalized path loss for Tx=1.6m. (a) 3 humans' activity. (b) 6 humans' activity.

The lognormal distribution parameters used to fit the data measurements are given in Table. 4.6.

Table 4.6 Lognormal distribution parameters

Antennas Height	3 HUMANS' ACTIVITY		6 HUMANS' ACTIVITY	
	μ	σ	μ	σ
Tx= 1m and Rx=1m	2.458	0.578	2.612	0.626
Tx= 1.3m and Rx=1m	2.504	0.531	2.847	0.551
Tx= 1.6m and Rx=1m	2.393	0.564	2.455	0.562

The following key figures summarize the normalized path loss values regarding all antenna heights and human activities based on the proposed empirical model:

•The mean path loss value does not change significantly when increasing the transmitter height for three humans' activity; however, the transmitter height is considered to be an important parameter for 6 humans' activities.

•The mean path loss differs for a maximum of 5dB when comparing an activity of 3 persons and an activity of 6 persons (Tx=1.3m), and remains the same for 1.6m case.

•The maximum level of path loss observed, for the three humans' activity is recorded as 27dB (Tx= 1m and 1.3m), and 35dB for six humans' activity (Tx= 1.3m).

•The least path loss levels are observed to be when the transmitter is at 1.6m, with a different in range of 4 to 8dB when compared with Tx=1m and Tx=1.3m for six humans' activities.

CHAPTER 5

CONCLUSION

Human bodies are one of the main blockers of radio waves in 5G wireless systems using mm-Wave frequency bands. In this thesis, we presented a comprehensive literature survey of the existing human blockage models used for mm-Wave spectrum providing quantitative comparison. In this study, the human blockage measurements at 28GHz considering 3 different human models with various dimensions were performed. The blockage loss was analysed by considering the crossing orientation of the human body, as well as several transmitter antenna heights. The Fresnel diffraction human blockage model was used to predict the experimental measurements of the human blockage losses. The model was able to fit the measurements accurately and was found to be more precise than the GTD model. It was observed that the human height and width, along with the crossing orientation and transmitter height are the key parameters influencing the human blockage loss and must be taken into consideration when developing theoretical models. Small-scale fading statistics of received signal was also measured for indoor short range communication links at 28GHz in a typical indoor office environment. A range of 3 to 6 humans' activities for 3 different antenna heights were investigated. It was found that in NLOS scenarios the fading can be described as a log-normal distribution, whereas the blockage duration can be described in terms of an exponential distribution. It is believed that the results reported in this thesis will be vital in designing mm-Wave spectrum based wireless systems that can overcome the extremely large fades caused by human blockages. Also, the reported results on the small scale fading statistics will aid the 5G/B5G wireless community on developing beam scanning techniques and handoff algorithms for mm-Wave communication systems.

REFERENCE

[1] T. S. Rappaport, Y. Xing, G. R. MacCartney, A. F. Molisch, E. Mellios, and J. Zhang, "Overview of millimeter wave communications for fifth-generation (5G) wireless networks—With a focus on propagation models" *IEEE Transactions on antennas and propagation*, vol. 65, pp. 6213-6230, 2017.

[2] T. S. Rappaport, S. Sun, R. Mayzus, H. Zhao, Y. Azar, K. Wang, et al., "Millimeter wave mobile communications for 5G cellular: It will work!" *IEEE access*, vol. 1, pp. 335-349, 2013.

[3] T. S. Rappaport, G. R. MacCartney, S. Sun, H. Yan, and S. Deng, "Small-scale, local area, and transitional millimeter wave propagation for 5G communications" *IEEE Transactions on Antennas and Propagation*, vol. 65, pp. 6474-6490, 2017.

[4] X. Wu, C.-X. Wang, J. Sun, J. Huang, R. Feng, Y. Yang, et al., "60-GHz millimeter-wave channel measurements and modeling for indoor office environments" *IEEE Transactions on Antennas and Propagation*, vol. 65, pp. 1912-1924, 2017.

[5] G. R. Maccartney, T. S. Rappaport, S. Sun, and S. Deng, "Indoor office wideband millimeter-wave propagation measurements and channel models at 28 and 73 GHz for ultra-dense 5G wireless networks" *IEEE access*, vol. 3, pp. 2388-2424, 2015.

[6] A. Kara, "Human body shadowing variability in short-range indoor radio links at 3–11 GHz band" *International journal of electronics*, vol. 96, pp. 205-211, 2009.

[7] M. Gapeyenko, A. Samuylov, M. Gerasimenko, D. Moltchanov, S. Singh, M. R. Akdeniz, et al., "On the temporal effects of mobile blockers in urban millimeter-wave cellular scenarios" *IEEE Transactions on Vehicular Technology*, vol. 66, pp. 10124-10138, 2017.

[8] A. Kara and H. L. Bertoni, "Effect of people moving near short-range indoor propagation links at 2.45 GHz" *Journal of Communications and Networks*, vol. 8, pp. 286-289, 2006.

[9] M. Rumney, P. Kyösti, and L. Hentila, "3GPP channel model developments for 5G NR requirements and testing" *in 2018 12th European Conference on Antennas and Propagation (EuCAP)*, 2018, pp. 1-5.

[10] U. T. Virk and K. Haneda, "Modeling human blockage at 5G millimeter-wave frequencies" *IEEE Transactions on Antennas and Propagation*, vol. 68, pp. 2256-2266, 2019.

[11] W. Qi, J. Huang, J. Sun, Y. Tan, C.-X. Wang, and X. Ge, "Measurements and modeling of human blockage effects for multiple millimeter wave bands" *in 2017 13th International Wireless Communications and Mobile Computing Conference (IWCMC)*, 2017, pp. 1604-1609.

[12] G. R. MacCartney, S. Deng, S. Sun, and T. S. Rappaport, "Millimeter-wave human blockage at 73 GHz with a simple double knife-edge diffraction model and extension for directional antennas" *in 2016 IEEE 84th Vehicular Technology Conference (VTC-Fall)*, 2016, pp. 1-6.

[13] K. Akimoto, S. Kameda, M. Motoyoshi, and N. Suematsu, "Measurement of human body blocking at 60 GHz for inter-network interference of mmWave WBAN" *in 2017 IEEE Asia Pacific Microwave Conference (APMC)*, 2017, pp. 472-475.

[14] M. Peter, M. Wisotzki, M. Raceala-Motoc, W. Keusgen, R. Felbecker, M. Jacob, et al., "Analyzing human body shadowing at 60 GHz: Systematic wideband MIMO measurements and modeling approaches" *in 2012 6th European Conference on Antennas and Propagation (EUCAP)*, 2012, pp. 468-472.

[15] M. Jacob, S. Priebe, R. Dickhoff, T. Kleine-Ostmann, T. Schrader, and T. Kurner, "Diffraction in mm and sub-mm wave indoor propagation channels" *IEEE Transactions on Microwave Theory and Techniques*, vol. 60, pp. 833-844, 2012.

[16] M. Jacob, S. Priebe, T. Kürner, M. Peter, M. Wisotzki, R. Felbecker, et al., "Fundamental analyses of 60 GHz human blockage" *in 2013 7th European Conference on Antennas and Propagation (EuCAP)*, 2013, pp. 117-121.

[17] P. Karadimas, B. Allen, and P. Smith, "Human body shadowing characterization for 60-GHz indoor short-range wireless links" *IEEE Antennas and Wireless Propagation Letters*, vol. 12, pp. 1650-1653, 2013.

[18] J. S. Lu, D. Steinbach, P. Cabrol, and P. Pietraski, "Modeling human blockers in millimeter wave radio links" *ZTE communications*, vol. 10, pp. 23-28, 2012.

[19] C. Gustafson and F. Tufvesson, "Characterization of 60 GHz shadowing by human bodies and simple phantoms" *in 2012 6th European Conference on Antennas and Propagation (EUCAP)*, 2012, pp. 473-477.

[20] C.-M. Li, P.-Y. Lee, and P.-J. Wang, "Measurements of Human Body Attenuation and Dual Polarized Diversity Gain for 38 GHz Millimeter-Wave Channel" *Wireless Personal Communications*, pp. 1-13, 2021.

[21] X. Chen, L. Tian, P. Tang, and J. Zhang, "Modelling of human body shadowing based on 28 GHz indoor measurement results" *in 2016 IEEE 84th vehicular technology conference (VTC-Fall)*, 2016, pp. 1-5.

[22] T. Choi, C. U. Bas, R. Wang, S. Hur, J. Park, J. Zhang, et al., "Measurement based directional modeling of dynamic human body shadowing at 28 GHz" *in 2018 IEEE Global Communications Conference (GLOBECOM)*, 2018, pp. 1-6.

[23] B. T. Ahmed, "Human Body Shadowing at 28 GHz" *Wireless Personal Communications*, vol. 110, pp. 621-635, 2020.

[24] Y. Dalveren, G. Karatas, M. Derawi, and A. Kara, "A Simple Propagation Model to Characterize the Effects of Multiple Human Bodies Blocking Indoor Short-Range Links at 28 GHz" *Electronics*, vol. 10, p. 305, 2021.

[25] Y. Dalveren, A. H. Alabish, and A. Kara, "A simplified model for characterizing the effects of scattering objects and human body blocking indoor links at 28 GHz" *IEEE Access*, vol. 7, pp. 69687-69691, 2019.

[26] S. Collonge, G. Zaharia, and G. E. Zein, "Influence of the human activity on wide-band characteristics of the 60 GHz indoor radio channel" *IEEE Transactions on Wireless Communications*, vol. 3, pp. 2396-2406, 2004.

[27] A. Angles-Vazquez, E. Carreno, and L. S. Ahumada, "Modeling the effect of pedestrian traffic in 60-GHz wireless links" *IEEE Antennas and Wireless Propagation Letters*, vol. 16, pp. 1927-1931, 2017.

[28] C. Slezak, V. Semkin, S. Andreev, Y. Koucheryavy, and S. Rangan, "Empirical

effects of dynamic human-body blockage in 60 GHz communications" *IEEE Communications Magazine*, vol. 56, pp. 60-66, 2018.

[29] L. A. Fierro, E. C. Maggi, A. A. Vazquez, and D. Schkolnik, "Empirical Results for Human-Induced Shadowing Events for Indoor 60 GHz Wireless Links" *IEEE Access*, vol. 8, pp. 44522-44533, 2020.

[30] M. Nakamura, M. Sasaki, and Y. Takatori, "Human body shadowing at 26.4 and 66.5 GHz in an indoor environment" *in 2018 IEEE International Symposium on Antennas and Propagation & USNC/URSI National Radio Science Meeting*, 2018, pp. 757-758.

[31] M. Jacob, S. Priebe, T. Kürner, M. Peter, M. Wisotzki, R. Felbecker, et al., "Extension and validation of the IEEE 802.11 ad 60 GHz human blockage model" *in 2013 7th European Conference on Antennas and Propagation (EuCAP)*, 2013, pp. 2806-2810.

[32] M. Jacob, S. Priebe, A. Maltsev, A. Lomayev, V. Erceg, and T. Kürner, "A ray tracing based stochastic human blockage model for the IEEE 802.11 ad 60 GHz channel model" *in Proceedings of the 5th European Conference on Antennas and Propagation (EUCAP)*, 2011, pp. 3084-3088.

[33] D. Cassioli and N. Rendevski, "A statistical model for the shadowing induced by human bodies in the proximity of a mmWaves radio link" *in 2014 IEEE International Conference on Communications Workshops (ICC)*, 2014, pp. 14-19.

[34] X. Zhao, Q. Wang, S. Li, S. Geng, M. Wang, S. Sun, et al. "Attenuation by human bodies at 26-and 39.5-GHz millimeter wavebands" *IEEE Antennas and Wireless Propagation Letters*, vol. 16, pp. 1229-1232, 2016.

[35] T. S. Rappaport, "Wireless communications: principles and practice" *in IEEE Press*, 1st ed., vol. 2, 1996.

[36] G. L. James, "Geometrical theory of diffraction for electromagnetic waves" *in IET*, 1st ed., vol. 1, 1986.

[37] M. Ghaddar, L. Talbi, T. A. Denidni, and A. Sebak, "A conducting cylinder for modeling human body presence in indoor propagation channel" *IEEE Transactions on*

Antennas and Propagation, vol. 55, pp. 3099-3103, 2007.

[38] M. Ghaddar, L. Talbi, and T. Denidni, "Human body modelling for prediction of effect of people on indoor propagation channel" *Electronics letters*, vol. 40, pp. 1592-1594, 2004.